ACTA MYOL 2023;XLII:43-52
doi: 10.36185/2532-1900-339

ORIGINAL ARTICLES

The atrial and ventricular myocardial proteome of end-stage lamin heart disease

Constantin-Cristian Topriceanu* [1,2,3], Mashael Alfarih* [1,2], Alun D Hughes[1,2], Hunain Shiwani[3], Fiona Chan[1,2], Saidi A. Mohiddin[4], William Moody[5,6], Richard P. Steeds[5,6], Benjamin O'Brien[7,8,9,10], Jakob Vowinckel[11], Petros Syrris[2], Caroline Coats[12], Stephen Pettit[13], Eloisa Arbustini[14], James C. Moon[2,3], Gabriella Captur[1,2,15] **Authors contributed equally*

[1] UCL MRC Unit for Lifelong Health and Ageing, University College London, London, UK; [2] UCL Institute of Cardiovascular Science, University College London, London, UK; [3] Cardiac MRI Unit, Barts Heart Centre, London, UK; [4] Biomedical Research Unit at Barts, Barts Heart Center, London, UK; [5] Centre for Cardiovascular Sciences, University of Birmingham, Birmingham, UK; [6] Department of Cardiology, The Queen Elizabeth Hospital Birmingham, UK; [7] Department of Perioperative Medicine, St. Bartholomew's Hospital, London, UK; [8] Department of Cardiac Anesthesiology and Intensive Care Medicine, German Heart Center, Berlin, Germany; [9] Department of Cardiac Anesthesiology and Intensive Care Medicine, Charité Berlin, Berlin, Germany; [10] Outcomes Research Consortium, Department of Outcomes Research, The Cleveland Clinic, Ohio, USA; [11] Biognosys AG, Schlieren, Switzerland; [12] Queen Elizabeth University Hospital, Glasgow, UK; [13] Advanced Heart Failure and Transplant Unit, Royal Papworth Hospital, Cambridge, UK; [14] Transplant Research Area and Centre for Inherited Cardiovascular Diseases, Department of Medical Sciences and Infectious Diseases, IRCCS San Matteo Hospital Foundation, Pavia, Italy; [15] The Royal Free Hospital, Centre for Inherited Heart Muscle Conditions, Cardiology Department, Pond Street, Hampstead, London, UK

Received: September 14, 2023
Accepted: October 2, 2023

Correspondence
Gabriella Captur
Consultant Cardiologist in Inherited Heart Muscle Conditions, Senior Clinical Lecturer, Institute of Cardiovascular Science, University College London, UK
E-mail: gabriella.captur@ucl.ac.uk

How to cite this article: Topriceanu CC, Alfarih M, Hughes AD, et al. The atrial and ventricular myocardial proteome of end-stage lamin heart disease.. Acta Myol 2023;42:43-52. https://doi.org/10.36185/2532-1900-339

Lamins A/C (encoded by *LMNA* gene) can lead to dilated cardiomyopathy (DCM). This pilot study sought to explore the postgenomic phenotype of end-stage lamin heart disease.

Consecutive patients with end-stage lamin heart disease (LMNA-group, n = 7) and ischaemic DCM (ICM-group, n = 7) undergoing heart transplantation were prospectively enrolled. Samples were obtained from left atrium (LA), left ventricle (LV), right atrium (RA), right ventricle (RV) and interventricular septum (IVS), avoiding the infarcted myocardial segments in the ICM-group. Samples were analysed using a discovery 'shotgun' proteomics approach.

We found that 990 proteins were differentially abundant between LMNA and ICM samples with the LA being most perturbed (16-fold more than the LV). Abundance of lamin A/C protein was reduced, but lamin B increased in LMNA LA/RA tissue compared to ICM, but not in LV/RV. Carbonic anhydrase 3 (CA3) was over-abundant across all LMNA tissue samples (LA, LV, RA, RV, and IVS) when compared to ICM. Transthyretin was more abundant in the LV/RV of LMNA compared to ICM, while sarcomeric proteins such as titin and cardiac alpha-cardiac myosin heavy chain were generally less abundant in RA/LA of LMNA. Protein expression profiling and enrichment analysis pointed towards sarcopenia, extracellular matrix remodeling, deficient myocardial energetics, redox imbalances, and abnormal calcium handling in LMNA samples.

Compared to ICM, end-stage lamin heart disease is a biventricular but especially a biatrial disease appearing to have an abundance of lamin B, CA3 and transthyretin, potentially hinting to compensatory responses.

Key words: lamin heart disease, proteomics, remodelling, compensatory expression

Introduction

Dilated cardiomyopathy (DCM) caused by mutations in the lamin A/C gene (*LMNA*) continues to be ranked clinically as one of the most severe forms of DCM because of its high propensity for sudden cardiac death and advanced heart failure [1].

The *LMNA* gene codes for lamin A and C, while the lamin B genes (*LMNB1* and *LMNB2)* code for lamins B1/B2 respectively, all of which are inner nuclear envelope support filaments [2]. To date, only *LMNA* and not *LMNB1/2* gene mutations are known to affect the heart causing lamin heart disease [2]. The genetic heterogeneity of patients with lamin heart disease translates into diverse cardiovascular disease trajectories ranging from asymptomatic with normal life expectancy, to premature morbidity and mortality with a variable risk of arrhythmias, sudden death or progression to end-stage heart failure [3]. Understanding the myocardial protein landscape of patients with end-stage lamin heart disease could provide novel pathophysiological insights into these diverse disease trajectories and unmask novel potentially druggable targets to alter or reverse disease progression. Mass spectrometry (MS) enables the accurate, precise, and reproducible measurement of proteins in tissues [4], but little is known about the myocardial protein landscape of the failing heart in lamin heart disease.

In this pilot study, we undertook discovery 'shotgun' MS [5] protein profiling of the myocardium focusing on patients with end-stage lamin heart disease at the time of transplantation and analysing myocardial samples from each of the four cardiac chambers.

Patients and methods

Study population

Study participants were consecutive end-stage DCM heart transplant candidates recruited from the Royal Papworth Hospital NHS Foundation Trust, Cambridge UK between 2017 and 2020. Samples were prospectively collected as part of the multi-centre study "The Deep phenotype of Lamin A/C cardiomyopathy" which received ethical approval from the London North Thames research ethics committee (REC 16/0661; NCT03860454; IRAS No: 210790). All procedures performed were in accordance with the ethical standards of the institutional and/or national research committee and with the 1964 Helsinki declaration and its later amendments or comparable ethical standards.

The etiology of the DCM was confirmed using whole exome sequencing (WES) of myocardial tissue samples and imaging, including pre-transplant echocardiography on all patients. In this study, we prospectively included carriers of DCM-causing *LMNA* mutations (LMNA group) and a comparator group of patients with ischaemic cardiomyopathy (ICM group) free of DCM-causing gene mutations. The left atrium (LA) left ventricle (LV), right atrium (RA), right ventricle (RV) and IVS were biopsied from the explanted hearts of both groups.

Sample harvesting

Myocardial specimens (each of length ≥ 2cm) were harvested fresh, immediately after cardiac explantation. For ICM samples, only non-infarcted myocardium was biopsied. Each excised tissue sample was placed in a separate container to avoid cross-contamination of sample material, and the container was then immediately submerged into liquid nitrogen thus flash freezing the sample which was subsequently stored in the -80°C freezer. Samples were shipped to the proteomics laboratory on dry ice at -80°C without any intervening freeze thaw cycles.

Whole exome sequencing

Myocardial samples pertaining to LMNA and ICM patients were studied by a massively parallel next generation sequencing method using a library that includes 19,055 genes obtained from RefSeq and advanced interpretation of cardiovascular diseases global panel genes. This method has a reported sensitivity and specificity > 99% for single-nucleotide variants and small insertion-deletions (≤ 20 bp) [6]. Briefly, DNA purification was performed using QIAsymphony SP®, Qiagen. Agilent SureSelect library kit was employed for library preparation. Agilent SureSelect kit was used to enrich zones of interest. Illumina HiSeq 1500 platform was subsequently utilized for sequencing [7].

Sample preparation from specimens to peptides

Unless otherwise stated, all chemicals were high purity grade and obtained from Sigma-Aldrich (Saint Louis, Missouri, US). Specimens were prepared using the Biognosys (Schlieren, Switzerland) optimized protocol which was previously described [8]. Firstly, specimens were lysed using Biognosys Denature Buffer. Then, proteins were reduced and alkylated in the dark using Biognosys Reduction and Alkylation solution for 1 hour at 37°C. Processed proteins were digested overnight to peptides at 37°C with trypsin (Promega, Madison Wisconsin, US) using a 1:50 protease to total protein ratio per sample. Peptides were desalted using an octadecyl carbon chain (C18) MicroSpin plate (The Nest Group, Ipswich, Massachusetts, US) and a SpeedVac system (Thermo Scientific, Waltham, Massachusetts, US). Peptides were suspended in 1% acetonitrile and 0.1% formic acid (solution A), and spiked with Biognosys iRT calibration kit. Peptide concentrations were determined using the ultraviolet visible (UV/VIS) spectrometer SPECTROstar Nano (BMG Labtech, Aylesbury, UK). Then, peptides were pooled according to the group (i.e., LMNA and ICM), and ammonium hydroxide added to the pools until a pH > 10 was reached to alkalinize the samples.

Peptide purification using high-pH reversed-phase chromatography

For LMNA and ICM samples, a high-pH reversed-phase chromatography (HPRP) using a C18-bonded silica column was employed for the purification of peptides with methodology previous described[8]. HRCP was performed at a flow of 0.8 ml/min in 20 minutes using a linear gradient of 1% to 40% acetonitrile (solution B) gradient in an ensemble of a Dionex™ UltiMate™ 3000 pump (Thermo Scientific, Waltham, Massachusetts, US) coupled with an Acquity UPLC CSH C18 Column (Waters PLC, Manchester UK). Fractions were collected every 30 seconds, pooled into 5 fractions, left to dry, resuspended in solution A, and normalized using the Biognosys® iRT calibration kit. Peptide concentrations were determined using the UV/VIS spectrometry as above.

Peptide spectral library generation using shotgun proteomics

Multidimensional LC combined with MS known as "shotgun proteomics" has a superior throughput and sensitivity when compared to classical approaches [9]. We used LC-MS/MS with data-dependent acquisition (DDA) for measurements in LMNA and ICM samples. Heart peptides (1µ) were injected into a C18-reversed phase column on an EASY-nLC™ (Thermo Scientific) nano-liquid chromatography system connected to a Q Exactive™ HF mass spectrometer equipped with a Nanospray Flex™ on source (all from Thermo Scientific). The LC solvents were: (1) solvent A (0.1% formic acid and 99.1% high purity water), and (2) solvent B (0.1% formic, 79.9% acetonitrile and 20% high purity water). Using a flow of 250 nL/min at 60° C, the non-linear gradient for solution C was as follows: (1) 1-59% in 55 mins, (2) 59-90% in 10s, (3) 90% in 8 mins, (4) 90%-100% in 10s, and (5) 1% 100% for 5 minutes [10]. We performed two MS scans: (1) MS1 (fragmentation of selected precursor) covering the 330-1650 m/z range with a resolution of 60,000, and (2) MS2 (ion spectral scan) covering the 4 m/z precursor isolation width with a resolution of 15000. The SpectroMine (Biognosys) search engine was used to analyze the MS data using a peptide/protein false discovery rate (FDR) of 0.01. The search engine is based on the Homo Sapiens UniProt to allow for up to 2 missed cleavages and peptide modifications such as N-terminal acetylation.

Data independent acquisition hyper-reaction mass spectrometry

In contrast to DDA LC-MS/MS, in hyper-reaction mass (HRM) data-independent acquisition (DIA) LC-MS/MS, MS1 represents a survey scan across all m/z windows while in MS2 the fragmentation of all precursors in each window occurs [11]. We performed the DDA LC-MS/MS using methodology described elsewhere [12]. The LC solvents and non-linear gradients were as above. The Spectronaut software (Biognosys) was used to analyze the HRM MS data using a peptide/protein FDR of 0.01. Measurements were normalized using local regression normalization [13].

Statistics and data analyses

Statistical analysis was performed in R 4.2.1. Distribution of data were assessed on histograms and normality checks were performed using the Shapiro-Wilk test. Continuous variables are expressed as mean ± 1 standard deviation (SD) or median (interquartile range) as appropriate; categorical variables, as counts and percent. Group differences for clinicodemographic characteristics were compared using Mann Whitney U-test, $\chi 2$ or Fisher's exact test as appropriate. A p-value < 0.05 was considered significant. All p-values were corrected for multiple testing using the q-value method [14].

We compared the concentration of proteins in LA, LV, RA, RV and IVS between the LMNA and ICM groups. A protein differently abundant is referred to as a "candidate". The following thresholds were applied for candidate identification: (1) absolute average log 2 ratio > 0.58 (equivalent to a 1.5x fold increase), and (2) q-value < 0.05. Since a higher q-value means that the protein would pass a more restrictive FDR cut-off, differentially abundant proteins were ranked based on q-value.

Principal component analysis [15] (PCA) was performed to visualize dataset variation, and to provide separation of tissue provenance (i.e., LA, LV, RA, RV and IVS) and sample group (i.e., LMNA and ICM). A gene ontology (GO) enrichment analysis [16] was performed using Spectronaut and a gene association file provided by the European Bioinformatics Institute (EBI). Biological processes, cellular components and molecular function GO categories with > 2 members were considered.

Results

Participant characteristics including *LMNA* mutation details, are presented in Table I. Among the 7 LMNA participants, 5 had missense and 2 nonsense mutations. There were no statistically significant differences in terms of demographics, the presence of co-morbidities, current medications, blood chemistry biomarkers and echocardiography metrics between LMNA and ICM groups.

Table I. Participant characteristics.

Characteristics	LMNA (n = 7)	ICM (n = 7)	p-value*
Demographic			
Age, years	42 (39.0, 43.4)	52 (48.0, 60.5)	0.306
Sex, Males	4 (57.1%)	6 (85.7%)	0.554
Body Mass Index (kg/m^2)	28.5 (26.0, 29.3)	26.1 (24.5, 28.7)	0.699
Ethnicity, White	5 (71.4%)	4 (57.1%)	0.503
Co-morbidities			
Smoking	0 (0.0%)	2 (28.6%)	0.445
Diabetes, yes	1 (14.3%)	2 (28.6%)	1.00
Atrial Fibrillation, yes	5 (71.4%)	1 (14.3%)	0.105
Stroke/TIA, yes	1 (14.3%)	1 (14.3%)	1.00
Chronic Kidney disease, yes	1 (14.3%)	1 (14.3%)	1.00
High cholesterol, yes	1 (14.3%)	3 (42.9%)	0.306
Medications			
Antiplatelet, yes	1 (14.3%)	7 (100%)	**0.020**
ACE inhibitor/ARB, yes	5 (71.4%)	7 (100%)	0.601
β-blocker, yes	5 (71.4%)	2 (28.6%)	0.621
SGLT-2 inhibitor, yes	3 (42.9%)	4 (57.1%)	0.896

continue ▶

Table I. *Follows.*

Characteristics	LMNA (*n* = 7)	ICM (*n* = 7)	*p*-value*
MRA	5 (71.4%)	7 (100%)	0.601
Blood thinner, yes	5 (71.4%)	4 (57.1%)	1.00
Calcium Channel blocker, yes	0 (0.0%)	2 (28.6%)	0.295
Diuretics, yes	3 (42.9%)	1 (14.3%)	0.836
Digoxin, yes	2 (28.6%)	4 (57.1%)	0.860
Echocardiography			
LVIDd, mm	60 (57.0, 62.0)	58.0 (51.0, 62.0)	0.807
LVIDs, mm	50 (46.3, 57.5)	45.0 (39.0, 51.5)	0.284
IVSd thickness, mm	8.4 (7.9, 8.5)	8.1 (8.0, 8.3)	0.807
LVPWTd, mm	7.9 (6.5, 8.6)	8.0 (7.7, 7.4)	0.625
Ejection Fraction (%)	24.3 (14.5, 32.3)	24.0 (20.3, 25.6)	0.876
LV mass (grams)	173.2 (161.1, 205.2)	209.0 (143.9, 209.9)	1.00
Medial E/e'	15.8 (11.6, 24.5)	15.0 (12.0, 18.1)	0.659
Lateral E/e'	8.6 (7.7, 11.7)	14.2 (14.0, 14.5)	0.333
TAPSE, cm	1.7 (1.2, 1.8)	1.5 (1.4, 1.7)	0.679
Blood chemistry and biomarkers			
NT-ProBNP	2824 (1279, 6822)	4671 (3158, 5508)	0.833
Hemoglobin:	122.0 (119.5, 131.0)	123.0 (106.0, 126.0)	0.807
Albumin	37.0 (31.0, 39.0)	39.0 (38.0, 39.0)	0.651
Total Bilirubin	16.0 (14.3, 18.5)	12.0 (7.0, 13.0)	0.389
Alanine Transaminase	40.5 (28.5, 51.0)	23.0 (17.0, 25.0)	0.08
Alkaline Phosphatase	96.0 (61.8, 133.8)	100.0 (96.0, 113.0)	1.00
Sodium	139.0 (138.5, 140.5)	138.0 (137.0, 139.0)	0.100
Potassium	4.2 (4.2, 4.5)	4.3 (4.2, 4.4)	1.00
Creatinine	129.0 (107.0, 164.5)	100.0 (98.5, 126.0)	0.833
Urea	10.4 (7.4, 14.6)	8.7 (7.8, 13.5)	0.931
Pathogenic variants by WES			
Subject #1	NP_733821.1:p.Arg62Cys NM_170707.3:c.184C > T	–	
Subject #2	NP_733821.1:p.Arg275Serfs*2 NM_170707.3:c.825_832delGCAGTCTG	–	
Subject #3	NP_733821.1:p.Leu479Alafs*73 NM_170707.3:c.1434_1435insG	–	
Subject #4	NP_733821.1:p.Arg190Trp NM_170707.3:c.568C > T	–	
Subject #5	NP_733821.1:p.Asp357His NM_170707.3:c.1069G > C	–	
Subject #6	NP_733821.1:p.Arg541His NM_170707.3:c.1622G > A	–	
Subject #7	NP_733821.1:p.Ala375Thr NM_170707.3:c.1123G > A	–	
Genetic variants by WES			
Total	34,318 (33,662; 36048)	33,133 (31,027; 34,004)	0.234
Exonic	19,947 (19,351; 20,813)	18,872 (17,546; 19,725)	0.181
Synonymous	10,060 (9788; 10,411)	9745 (9387, 10,256)	0.628
Non-synonymous	9300 (8985, 9776)	9159 (8517, 9484)	0.534
Nonsense/Frameshift	320 (315, 326)	310 (303, 315)	0.317
Insertion	121 (118, 131)	127 (123, 132)	0.295
Deletion	143 (142, 151)	146 (144, 147)	0.719
Intronic	12,720 (12,590; 13,488)	12,566 (12,339; 13,029)	0.534
Untranslated region	1673 (1644, 1691)	1708 (1694, 1734)	0.198

*Reported *p* values were derived using Mann Whitney U-test, χ^2 or Fisher's exact test as appropriate.
ACE, angiotensin converting enzyme; ARB, angiotensin receptor blocker; d, diastolic; LV, IVS, interventricular septum; left ventricle; LVID, LV internal diameter; LVPWT, LV posterior wall thickness; MRA, mineralocorticoid receptor antagonist; NT-ProBNP, N-terminal pro B-type natriuretic peptide; s, systolic; SGLT-2 = Sodium-glucose co-transporter-2; TAPSE, tricuspid annular plane systolic excursion; TIA, transient ischaemic attack.

Proteome-wide exploratory analysis

For each of the samples from explanted LMNA and ICM hearts, there were on average: (1) 3,811 proteins, (2) 41,935 peptides and (3) 58,302 peptide ion variants. In total 4,247 unique proteins available in all tissues in both LMNA and ICM groups were quantified. There were 633 differentially abundant proteins in the LA, 39 in LV, 181 in RA, 52 in RV and 85 in IVS between when comparing LMNA and ICM groups (Tab. II and Fig. 1). PCA highlighted the proteomic heterogeneity of atrial compared to ventricular samples but provided little separation between sample groups (i.e., LMNA and ICM, Supplementary Fig. S1).

Table II. Contingency table showing number of differentially abundant proteins between heart regions (RA, RV, LA, LV, IVS) and between groups (LMNA, ICM).

	LA_ICM	LA_LMNA	LV_ICM	LV_LMNA	RA_ICM	RA_LMNA	RV_ICM	RV_LMNA	IVS_DCM	IVS_LMNA
LA_ICM	N/A	**633**	156	185	307	443	194	224	318	242
LA_LMNA		N/A	721	723	177	83	848	948	1053	952
LV_ICM			N/A	**39**	530	779	39	64	132	77
LV_LMNA				N/A	484	769	59	28	166	33
RA_ICM					N/A	**181**	639	715	838	685
RA_LMNA						N/A	909	948	1077	944
RV_ICM							N/A	**52**	67	47
RV_LMNA								N/A	116	10
IVS_ICM									N/A	**85**
IVS_LMNA										N/A

For a protein to be regarded as differentially abundant (or a candidate protein), we used a 1.5x fold increase and a *q*-value < 0.05 as the threshold.
ICM, ischaemic dilated cardiomyopathy; IVS, interventricular septum; LA, left atrium; LMNA, lamin; LV, left ventricle; RA, right atrium; RV, right ventricle.

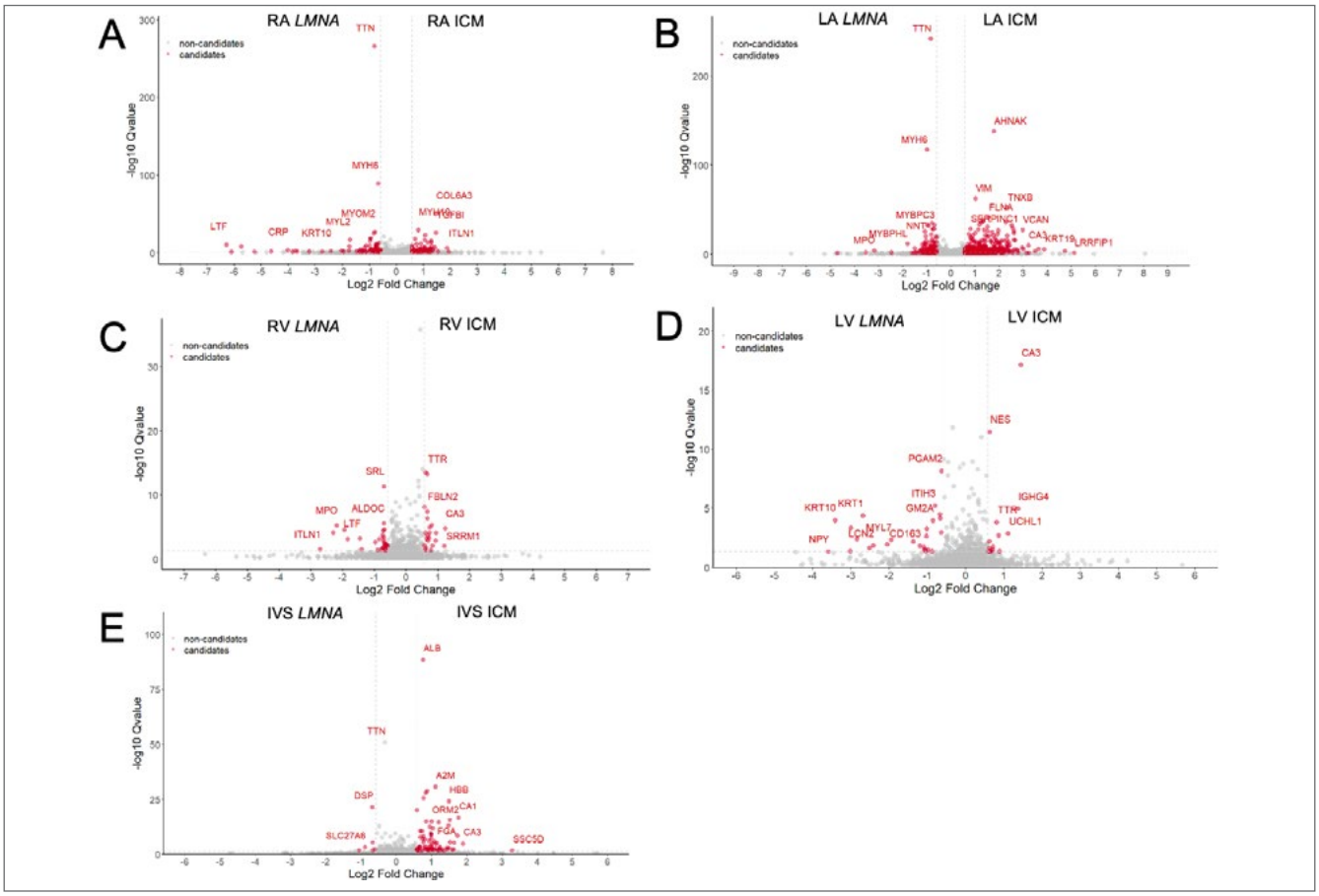

Figure 1. Volcano plots of differentially abundant proteins. There were 181 differentially abundant proteins in right atrium (A), 633 in the left atrium (B), 52 in right ventricle (C) 39 in left ventricle (D), and 85 in interventricular septum (E) when comparing LMNA and ICM samples. The most clinically relevant differentially abundant proteins are annotated in red. Atrial tissue showed a higher number of differentially abundant proteins (LMNA *vs* ICM) compared to ventricular tissue, but atrial tissue also showed a lower inter-individual variability.
ICM, ischaemic dilated cardiomyopathy; IVS, interventricular septum; LA, left atrium; LMNA, lamin; log, logarithm; LV, left ventricle; RA, right atrium; RV, right ventricle.

Lamins

LMNA and LMNB were detected in all samples from LMNA and ICM groups. Comparing $\log_2$ signal intensities between LMNA *vs* ICM groups, atrial myocardial LMNA was less abundant (LA: 21.8 *vs* 22.5, $p < 0.0001$; RA: 21.7 *vs* 22.4, $p < 0.0001$) while LMNB was more abundant (LA: 20.8 vs 19.9, $p < 0.0001$; RA: 20.6 *vs* 20.5, $p = 0.001$) with no such differences observed for either protein in the LV, RV, or IVS.

Differentially abundant proteins in atria

Box plots comparing the intensities of differentially abundant LA and RA proteins between LMNA and ICM samples are presented in Figure 2 and Supplementary Figure S2 respectively. Across both atria, sarcomeric proteins such (e.g., titin, alpha-cardiac myosin heavy chain 6 and 10, myosin light chain 2 etc.) were depleted in the LMNA compared to the ICM group. Indeed, the GO analysis suggested that the differentially abundant proteins in LMNA are involved in sarcomere organization, myosin filament assembly and cardiac muscle morphogenesis. In contrast, ECM proteins were both more and less differentially abundant (e.g., collagen, fibrillin). This is supported by the GO analysis which suggests that the differentially abundant proteins are involved in ECM remodeling processes (e.g., extracellular matrix organization, collagen fibril organization, fiber assembly etc.).

Differentially abundant proteins in the ventricles

Box plots comparing the intensities of differentially abundant LV, RV and IVS proteins between LMNA and ICM samples are presented in Figure 3 and Supplementary Figures S3 and S4 respectively. The number of the differentially abundant proteins differed based on tissue provenance (i.e., 39 in the LV, 52 in the RV and 85 in the IVS). Similarly, to the atria, ECM proteins were both more and less differentially abundant (e.g., collagen) and the GO analysis highlighted cellular processes involved in ECM remodeling (e.g., peptide cross-linking, regulation of cell-to-cell adhesion). In contrast to the RA/LA, transthyretin protein (TTR) was increased in the LV, RV as well as IVS. Although markers of redox imbalance and oxidative stress (e.g., cytochrome C oxidase subunit) appear to be more abundant in LMNA, pro-inflammatory proteins such as myeloperoxidase appeared less abundant. Moreover, compared to the ICM participants, glycolysis enzymes and calcium buffering proteins were less abundant in both the RV (e.g., aldolase C, sarcalumenin) and LV (e.g., phosphoglycerate mutase [PGAM], sarcalumenin).

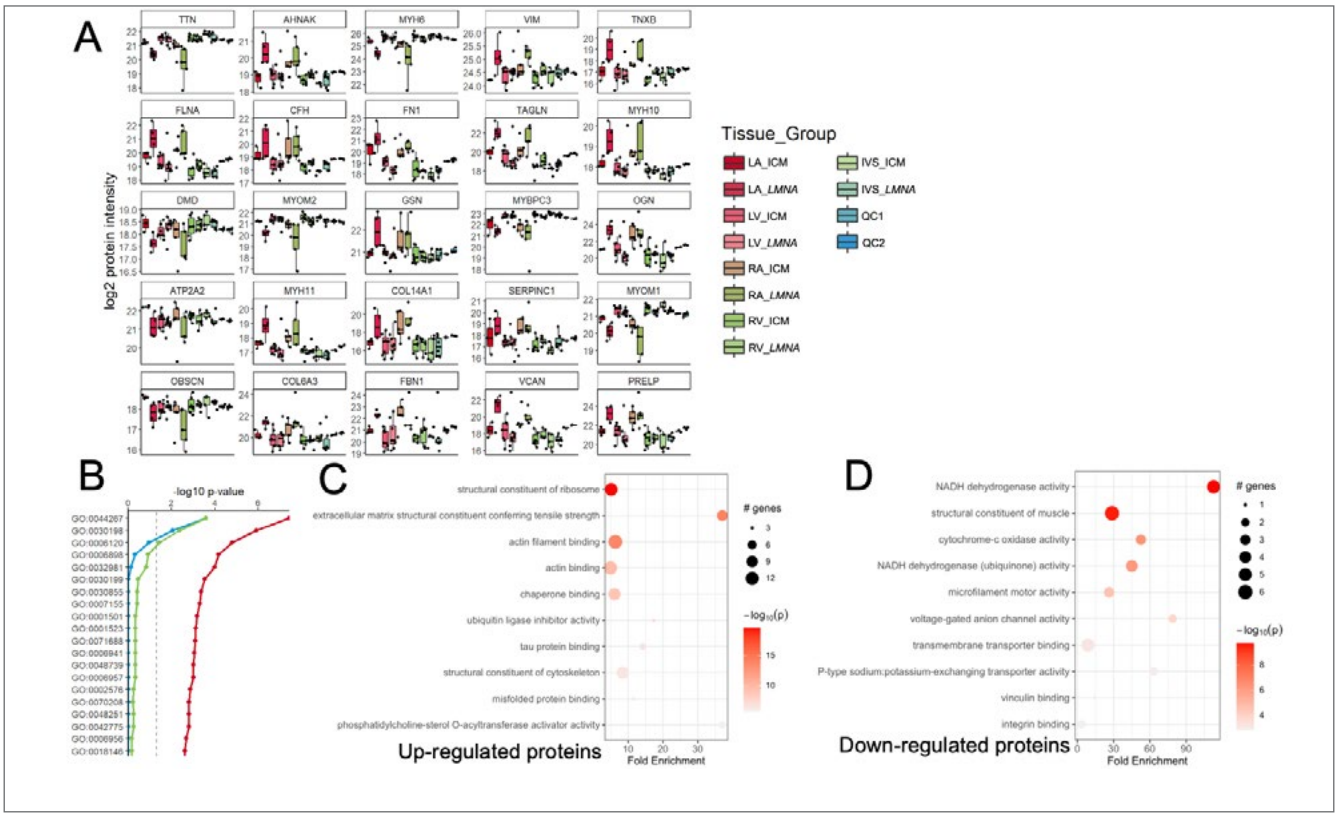

Figure 2. Differentially abundant left atrial myocardial proteins and their gene ontology. Box plots (A) comparing intensities of the top 25 LA proteins between *LMNA* and ICM based on *q*-value. Genes coding for the proteins rather than the proteins themselves are named. The top 20 enriched biological processes across the 633 differentially abundant LA proteins (more abundant proteins in C; less abundant proteins in D) are shown along with raw (red), Benjamini-Hochberg corrected (green) and Bonferroni corrected (blue) enrichment *p*-values and fold enrichment (in B).
GO, gene ontology; QC, quality control. Other abbreviations as in Figure 1.

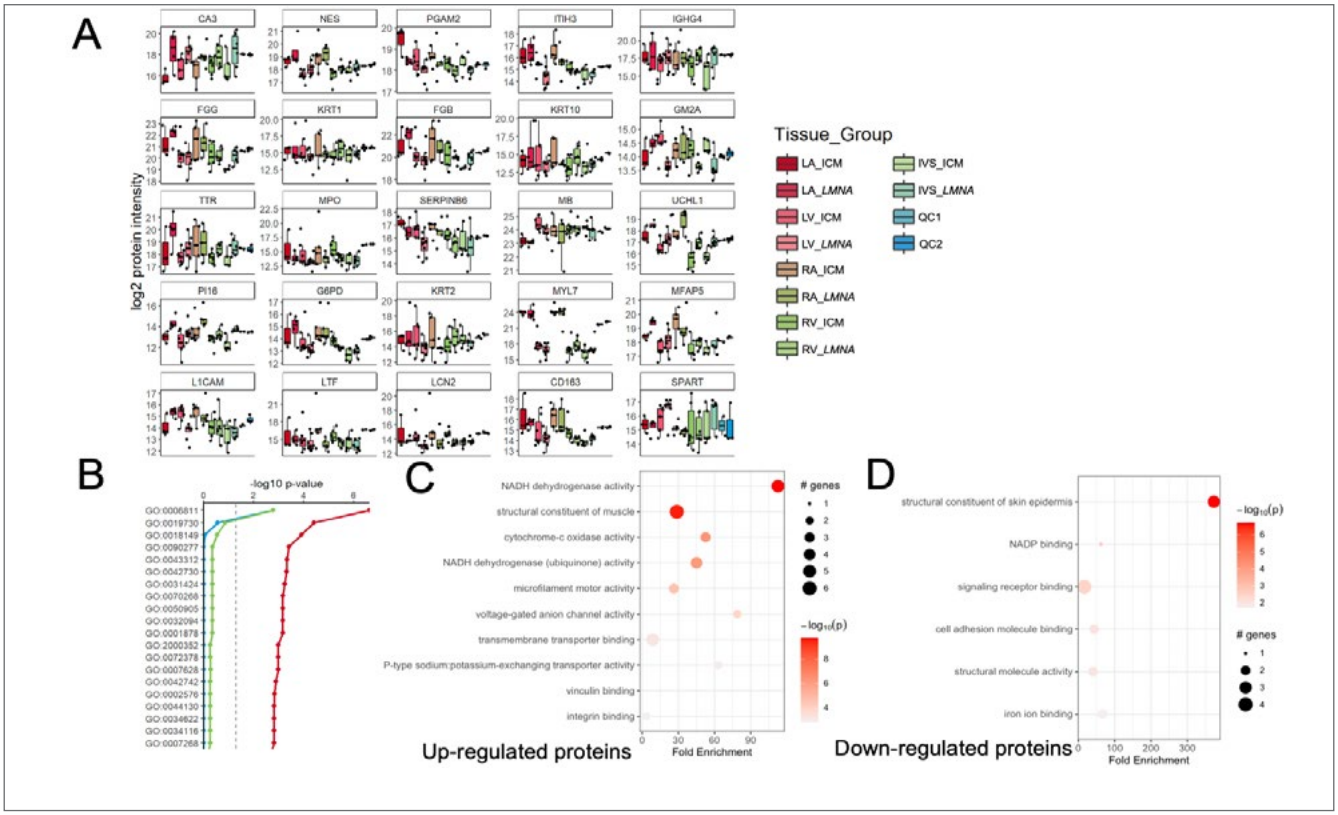

Figure 3. Differentially abundant left ventricular myocardial proteins and their gene ontology. Box plots (A) comparing intensities of the top differentially abundant 25 LV proteins between LMNA and ICM based on *q*-value. The top 20 enriched biological processes across the 39 differentially abundant LV proteins (more abundant proteins in C; less abundant proteins in D) are shown along with raw (red), Benjamini-Hochberg corrected (green) and Bonferroni corrected (blue) enrichment *p*-values and fold enrichment (in B).
Abbreviations as in Figures 1 and 2.

Discussion

In this exploratory analysis of the whole-heart myocardial proteome of end-stage lamin heart disease using mass spectrometry, we showed that compared to uninfarcted tissue from ICM hearts, the atrial proteome was more aberrant than the ventricular proteome (633 differentially abundant LA proteins compared to just 39 in LV). This suggests that lamin heart disease is not just a biventricular disease, but also and perhaps more importantly, a severe biatrial disease. Clinically, we already knew that there exists a clear atrial phenotype in lamin heart disease responsible for early onset atrial fibrillation/flutter or conduction system disease [17], but to our knowledge this is the first proteomics pilot highlighting the extent of atrial proteomic derangement.

We found aberrant ECM protein levels between LMNA and ICM samples across all cardiac chambers studied, suggesting global tissue remodeling in lamin heart disease compared to the more focal derangements expected with ICM. In general, pro-fibrotic fibrillar proteins such as collagen and filamin appear to be increased in LMNA that fits with the known burden of myocardial fibrosis typically identified by cardiovascular magnetic resonance in more than half of patients [18]. This fibrotic remodeling can serve as a pro-arrhythmogenic substrate [3,19,20].

TTR was increased in RV, IVS, and LV but not RA/LA samples from LMNA hearts. In health, TTR forms a tetramer complex acting as a transporter for retinol-binding protein and thyroxine. However, when it is overexpressed (e.g., TTR amyloidosis) it is deposited in the myocardium causing stiffness and diastolic dysfunction [21]. Building up from the structural hypothesis of lamin heart disease, it is plausible that excess TTR deposition may serve as a compensatory mechanism to provide stability to the weakened myocardial scaffolding network mitigating dilatation. Indeed, hypokinetic non-dilated cardiomyopathy is a recognized subphenotype [22] in *LMNA* mutation carriers raising the possibility that TTR abundance during this early disease stage may be one of the rescuing mechanisms. In a longitudinal study of patients with lamin heart disease it has been shown that the LV ejection fraction progressively declined even in the absence of LV dilation over a 5-year follow-up period [20,23], while diastolic dysfunction irrespective of systolic function, is a recognized feature perhaps driven by this TTR abundance [24]. So while TTR may provide some scaffolding protecting against volume-overload driven LV dilatation, this may come at the cost of diastolic dysfunction. Allowing enough TTR deposition for stability but preventing over-deposition and diastolic dysfunction may be a fine balance potentially achievable by repurposing amyloidosis drugs (e.g., tafamidis) for use in lamin heart disease.

Lamin A/C were decreased and lamin B1/B2 increased in both atria,

but not in LV/RV or IVS. Interestingly, while the RV/LV phenotype of lamin heart disease has been extensively described, information on the atrial phenotype is more scant [2]. Lamin B remains permanently farnesylated and attached to the nuclear membrane, while lamin A/C localizes closer to the nucleoplasm and creates a mesh providing a higher tensile strength [25]. Thus, the compensatory upregulation of lamin B may suffice to replace defective or scant lamin A/C in a low-pressure chamber such as the atria. Another consistent finding across the atria was the reduced abundance of sarcomeric proteins (especially titin) suggesting that lamin heart disease may be a sarcopenic state. Loss of muscle mass can of course reduce the contractile power leading to a lower cardiac output.

Glycolysis enzymes that use up large amounts of O_2 to drive glucose metabolism appear to be decreased in LMNA both in the RV (e.g., aldolase C) and LV (e.g., PGAM) compared to ICM samples. Yet we did not find any significant compensatory increase in analytes involved in fatty acid metabolism, suggesting profoundly deficient myocardial energetics in LMNA.

Markers of redox imbalance and oxidative stress were found to be increased in *LMNA* samples (e.g., cytochrome C oxidase subunit) compared to ICM. Indeed, LMNA participants had a higher number of both intronic and exonic mutations (Tab. I). As reactive oxygen species can damage the DNA, alter the tertiary/quaternary protein structure and cause lipid peroxidation, they can potentially accelerate lamin heart disease progression.

CA3 was abundant across all *LMNA* tissue samples (LA, LV, RA, RV, and IVS) when compared to ICM. Although other CA isoforms (e.g., CA2) are abundantly expressed in the myocardium, CA3 is usually only present in low levels in the heart [26]. A previous study found increased levels of CA3 in the serum of patients with DCM and heart failure compared to healthy volunteers [27]. Since CAs catalyze the conversion of H_2O and CO_2 into H_2CO_3 which dissociates to generate HCO_3^- and H^+, they work closely with the Na^+-H^+ (NHE) and Cl^- and HCO_3^- exchangers to regulate myocardial acid-base balance. As an acidic pH is negatively inotropic and predisposes to arrhythmias [28], overexpression of CA3 may represent a compensatory mechanism aimed at regulating intramyocardial pH. In addition, increased activity of CA3, increases the availability of H^+ meaning that more Na^+ can be removed by NHE. This reduces cytosolic Ca^{2+} as the Na^+/Ca^{2+} exchanger will be under-stimulated. A reduced cytosolic Ca^{2+} may help counter lamin heart disease development as described above. In other studies, myocardial CA3 was reportedly overexpressed in patients with hypertrophic cardiomyopathy [29], and CA inhibition was shown to attenuate hypertrophy in cell cultures [30].

Limitations

Although the sample size of our exploratory analysis is small, without healthy myocardial samples to serve as controls, these pilot data provide insights into the state of the myocardium in end-stage lamin-DCM compared to ICM. Findings may not be generalizable to the earlier or subclinical lamin heart disease states. As all participants had end-stage heart failure, polypharmacy could have confounded the proteomics expression although we go on to show that heart failure drug regimens between LMNA and ICM groups did not differ significantly except for the use of antiplatelets (Tab. I). Genetic heterogeneity between the patients within the LMNA group might have affected protein expression profiles (missense = 5; nonsense = 2) as could allelic imbalance and mosaic gene expression [31]. We had not included ethics to collect ECG data at the time of transplant for this study. However, LMNA participants were more likely to experience arrhythmias, which in itself could have confounded the myocardial protein abundance. We acknowledge that there are proteomics contributions arising from fibroblasts and endothelial cells in addition to the cardiomyocytes, but subcellular fractionation was not undertaken in this study. Although GO enrichment analysis highlighted pathways potentially involved in *LMNA* DCM, drawing mechanistic conclusions from a list of pathways has inherent limitations. All available tissue samples were used for proteomics with no residual, meaning that further analyses (e.g., western blots, histology) cannot be pursued. Lastly, the DNA samples were no longer available, so evaluating whether LMNA participants accumulated more mutations could not be explored.

Conclusion

Compared to ICM, end-stage lamin heart disease is a biventricular but especially a biatrial disease appearing to have an abundance of lamin B, CA3 and transthyretin, potentially hinting to compensatory responses.

Conflict of interest statement

The views expressed in this article are those of the authors who declare that they have no conflict of interest.

Funding

This work was funded by the Barts Charity HeartOME1000 Grant (MGU0427/G-001411). G.C. is supported by British Heart Foundation (MyoFit46 Special Programme Grant SP/20/2/34841), the National Institute for Health Research Rare Diseases Translational Research Collaboration (NIHR RD-TRC) and by the NIHR UCL Hospitals Biomedical Research Centre. J.C.M. is directly and indirectly supported by the UCL Hospitals NIHR BRC and Biomedical Research Unit at Barts Hospital respectively. AH receives support from the British Heart Foundation, the Economic and Social Research Council (ESRC), the Horizon 2020 Framework Programme of the European Union, the National Institute on Aging, the National Institute for Health Research University College London Hospitals Biomedical Research Centre, the UK Medical Research Council and works in a unit that receives support from the UK Medical Research Council.

Role of the funding source

None of the funders was involved in the study design, the collection, the analysis, the interpretation of the data, and in the decision to submit the article for publication.

Authors' contributions

All authors contributed significantly to the design, implementation, analysis, interpretation, and manuscript writing. The corresponding author attests that all listed authors meet the authorship criteria and that no others meeting the criteria have been omitted.

Data and code availability

Upon publication, the final R scripts will be made publicly available on GitHub. The MS proteomics data have been deposited to the ProteomeXchange Consortium (http://proteomecentral.proteomexchange.org) via the PRIDE partner repository (Accession number: PXD040488).

Ethical consideration

This proteomics sub-study, part of "The Deep phenotype of Lamin A/C cardiomyopathy" (NCT03860454) received ethical approval from the London North Thames Research Ethics Committee (Research Ethics Committee [REC] reference 16/0661;UK Integrated Research Application System number: 210790). All participants provided written informed consent and conformed to the Declaration of Helsinki (fifth revision, 2000).

References

1 Arbelo E, Protonotarios A, Gimeno JR, et al. 2023 ESC Guidelines for the management of cardiomyopathies. Eur Heart J 2023;44:3503-3626. https://doi.org/10.1093/eurheartj/ehad194

2 Captur G, Arbustini E, Bonne G, et al. Lamin and the heart. Heart 2018;104:468-479. https://doi.org/10.1136/heartjnl-2017-312338.

3 van Berlo JH, de Voogt WG, van der Kooi AJ, et al. Meta-analysis of clinical characteristics of 299 carriers of LMNA gene mutations: do lamin A/C mutations portend a high risk of sudden death? J Mol Med (Berl) 2005;83:79-83. https://doi.org/10.1007/s00109-004-0589-1

4 Buchberger AR, DeLaney K, Johnson J, et al. Mass spectrometry imaging: a review of emerging advancements and future insights. Anal Chem 2018;90:240-265. https://doi.org/10.1021/acs.analchem.7b04733

5 Zhang Y, Fonslow BR, Shan B, et al. Protein Analysis by Shotgun/Bottom-up Proteomics. Chemical Rev 2013;113:2343-2394. https://doi.org/10.1021/cr3003533

6 Guo X, Fan C, Wang Y, et al. Genetic anticipation in a special form of hypertrophic cardiomyopathy with sudden cardiac death in a family with 74 members across 5 generations. Medicine 2017;96:e6249-e6249. https://doi.org/10.1097/MD.0000000000006249

7 Andor M, Suciu M, Abukabda A. Cardiovascular risk factors in pathology. Abukabda A, Suciu A, Andor M, eds. London: IntechOpen; 2021.

8 Pandya NJ, Meier S, Tyanova S, et al. A cross-species spatiotemporal proteomic analysis identifies UBE3A-dependent signaling pathways and targets. Mol Psychiatry 2022;27:2590-2601. https://doi.org/10.1038/s41380-022-01484-z

9 Zhang X, Fang A, Riley CP, et al. Multi-dimensional liquid chromatography in proteomics - A review. Anal Chim Acta 2010;664:101-113. https://doi.org/10.1016/j.aca.2010.02.001

10 Scheltema RA, Hauschild J-P, Lange O, et al. The Q Exactive HF, a Benchtop Mass Spectrometer with a Pre-filter, High-performance quadrupole and an ultra-high-field orbitrap analyzer. Mol Cell Proteomics 2014;13:3698-3708. https://doi.org/10.1074/mcp.M114.043489

11 Krasny L, Huang PH. Data-independent acquisition mass spectrometry (DIA-MS) for proteomic applications in oncology. Mol Omics 2021;17:29-42. https://doi.org/10.1039/d0mo00072h

12 Bruderer R, Bernhardt OM, Gandhi T, et al. Optimization of experimental parameters in data-independent mass spectrometry significantly increases depth and reproducibility of results. Mol Cell Proteomics 2017;16:2296-2309. https://doi.org/10.1074/mcp.RA117.000314

13 Callister SJ, Barry RC, Adkins JN, et al. Normalization approaches for removing systematic biases associated with mass spectrometry and label-free proteomics. J Proteome Res 2006;5:277-286. https://doi.org/10.1021/pr050300l

14 Storey JD, Tibshirani R. Statistical significance for genomewide studies. PProc Natl Acad Sci U S A 2003;100:9440-9445. https://doi.org/10.1073/pnas.1530509100

15 Ding C, He X. Cluster Structure of K-means Clustering via Principal Component Analysis. Paper/Poster presented 2004, Berlin, Heidelberg.

16 Tomczak A, Mortensen JM, Winnenburg R, et al. Interpretation of biological experiments changes with evolution of the Gene Ontology and its annotations. Sci Rep 2018;8:5115-5110. https://doi.org/10.1038/s41598-018-23395-2

17 van Rijsingen IAW, Arbustini E, Elliott PM, et al. Risk Factors for Malignant Ventricular Arrhythmias in Lamin A/C Mutation Carriers A European Cohort Study. JJ Am Coll Cardiol 2012;59:493-500. https://doi.org/10.1016/j.jacc.2011.08.078

18 Holmström M, Kivistö S, Heliö T, et al. Late gadolinium enhanced cardiovascular magnetic resonance of lamin A/C gene mutation related dilated cardiomyopathy. J Cardiovasc Magn Reson 2011;13:30-30. https://doi.org/10.1186/1532-429X-13-30

19 Brodt CMD, Siegfried JDMSCGC, Hofmeyer MMD, et al. Temporal relationship of conduction system disease and ventricular dysfunction in LMNA cardiomyopathy. J Card Fail 2013;19:233-239. https://doi.org/10.1016/j.cardfail.2013.03.001

20 Hasselberg NE, Haland TF, Saberniak J,et al. Lamin A/C cardiomyopathy: young onset, high penetrance, and frequent need for heart transplantation. Eur Heart J 2018;39:853-860. https://doi.org/10.1093/eurheartj/ehx596

21 Koike H, Katsuno M. Transthyretin Amyloidosis: Update on the Clinical Spectrum, Pathogenesis, and Disease-Modifying Therapies. Neurol Ther 2020;9:317-333. https://doi.org/10.1007/s40120-020-00210-7

22 Taylor MRG, Fain PR, Sinagra G, et al. Natural history of dilated cardiomyopathy due to lamin A/C gene mutations. J Am Coll Cardiol 2003;41:771-780. https://doi.org/10.1016/S0735-1097(02)02954-6

23 Skjølsvik ET, Haugen Lie Ø, Chivulescu M, et al. Progression of cardiac disease in patients with lamin A/C mutations. Eur Heart J Cardiovasc Imaging 2022;23:543-550. https://doi.org/10.1093/ehjci/jeab057

24 Raman SV, Sparks EA, Baker PM, et al. Mid-myocardial fibrosis by Cardiac magnetic resonance in patients with lamin A/C Cardiomyopathy: possible substrate for diastolic dysfunction. J Cardiovasc Magn Reson 2007;9:907-913. https://doi.org/10.1080/10976640701693733

25 Nmezi B, Xu J, Fu R, et al. Concentric organization of A- and B-type lamins predicts their distinct roles in the spatial organization and stability of the nuclear lamina [published correction appears in PNAS Plus]. Proc Natl Acad Sci U S A 2019;116:4307-4315. https://doi.org/10.1073/pnas.1810070116

26 Harju A-K, Bootorabi F, Kuuslahti M, et al. Carbonic anhydrase III: A neglected isozyme is stepping into the limelight. J Enzyme Inhib Med Chem 2013;28:231-239. https://doi.org/10.3109/14756366.2012.700640

27 Su H, Hu K, Liu Z, et al. Carbonic anhydrase 2 and 3 as risk biomarkers for dilated cardiomyopathy associated heart failure. Ann Palliat Med 2021;10:12554-12565. https://doi.org/10.21037/apm-21-3561

28 Nisbet AM, Burton FL, Walker NL, et al. Acidosis slows electrical conduction through the atrio-ventricular node. Front Physiol 2014;5:233-233. https://doi.org/10.3389/fphys.2014.00233

29 Coats CJ, Heywood WE, Virasami A, et al. Proteomic analysis of the myocardium in hypertrophic obstructive cardiomyopathy. Circ Genom Precis Med 2018;11:e001974. https://doi.org/10.1161/CIRCGEN.117.001974

30 Alvarez BV, Quon AL, Mullen J, et al. Quantification of carbonic anhydrase gene expression in ventricle of hypertrophic and failing human heart. BMC Cardiovasc Disord 2013;13:2-2. https://doi.org/10.1186/1471-2261-13-2

31 Kraft T, Montag J, Radocaj A, et al. Hypertrophic cardiomyopathy: cell-to-cell imbalance in gene expression and contraction force as trigger for disease phenotype development. Circ Res 2016;119:992-995. https://doi.org/10.1161/CIRCRESAHA.116.309804

Supplementary materials

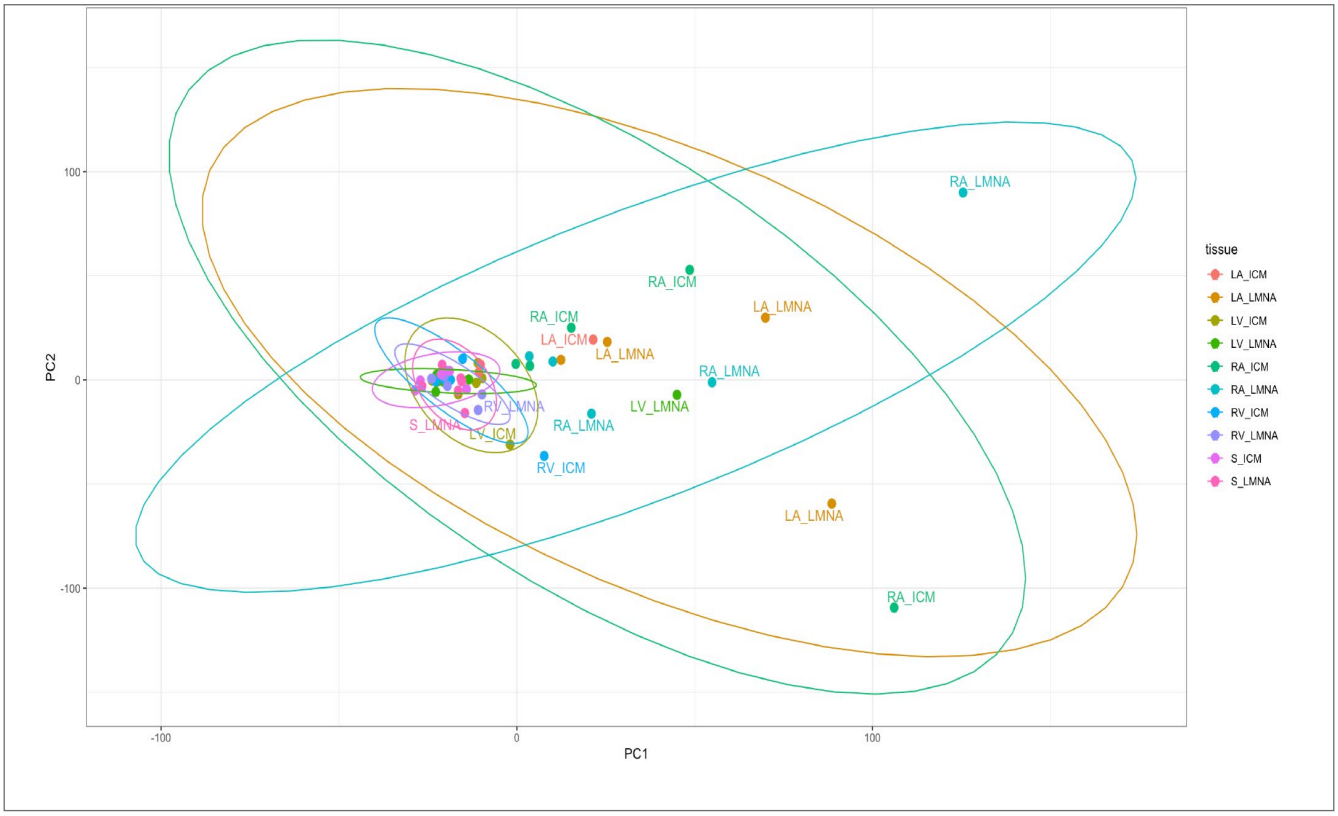

Supplementary Figure S1. Principal component analysis of the atrial and ventricular proteome. PCA was performed to visualize dataset variation, and to provide separation of tissue provenance (i.e., LA, LV, RA, RV or S) and sample group (i.e., LMNA or CTRL). Whilst 40.7% of the variance was explained by PC1 + PC2, PCA provided little separation between the samples.
CTRL, control (i.e., ischaemic dilated cardiomyopathy [ICM]); LA, left atrium; LMNA, lamin; LV, left ventricle; PC, principal component; PCA, principal component analysis; RA, right atrium; RV, right ventricle and S, septum (i.e., interventricular septum).

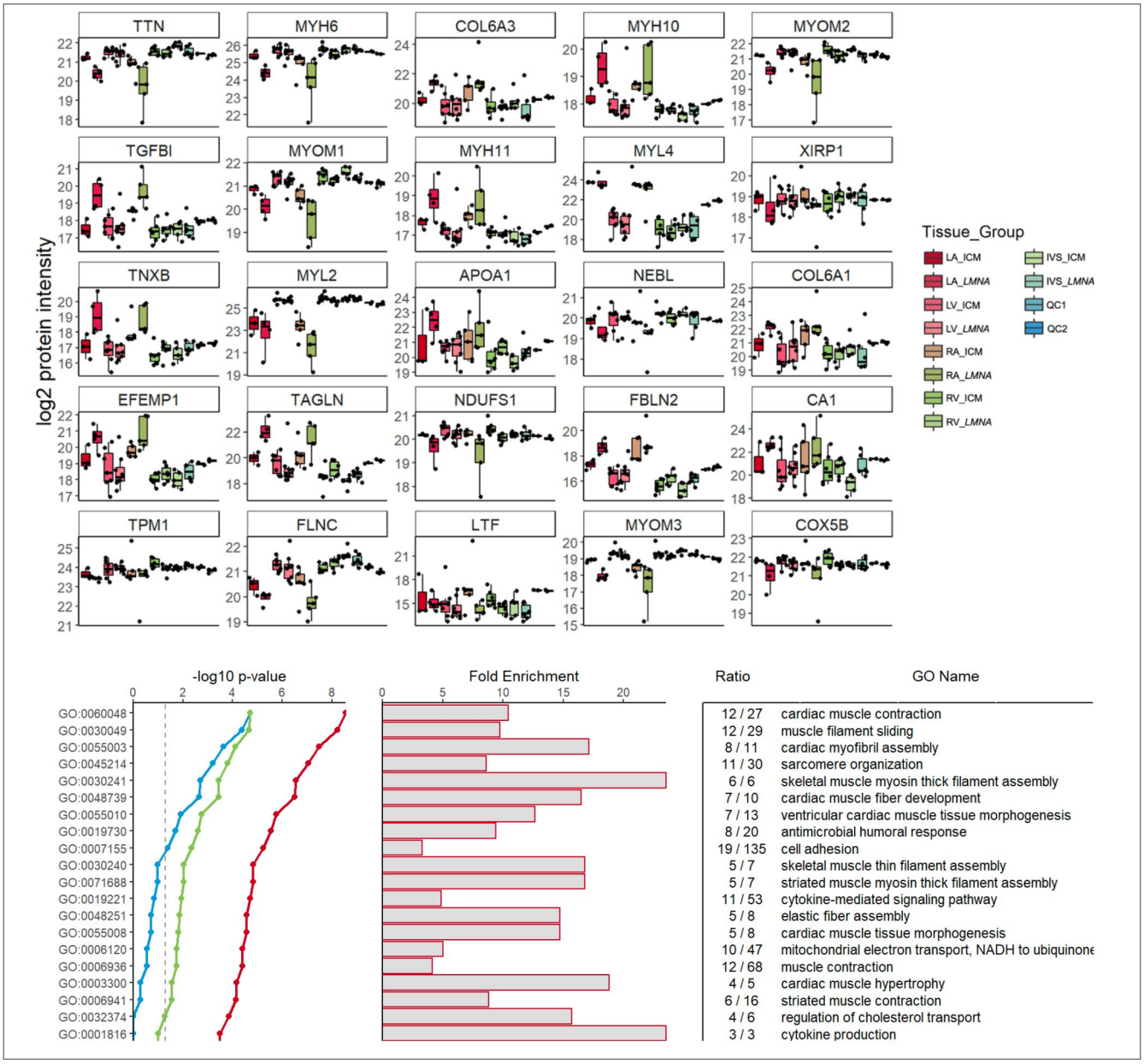

Supplementary Figure S2. Right atrial myocardial proteins and their gene ontology. Box plots (**top panel**) comparing intensities of the top 25 differentially abundant RA proteins between LMNA and ICM based on *q*-value. The top 20 enriched biological processes across the 181 proteins are presented (**bottom panel**) along with enrichment *p*-values and fold enrichment.
GO, gene ontology; QC, quality control. Other abbreviations as in Supplementary Figure S1.

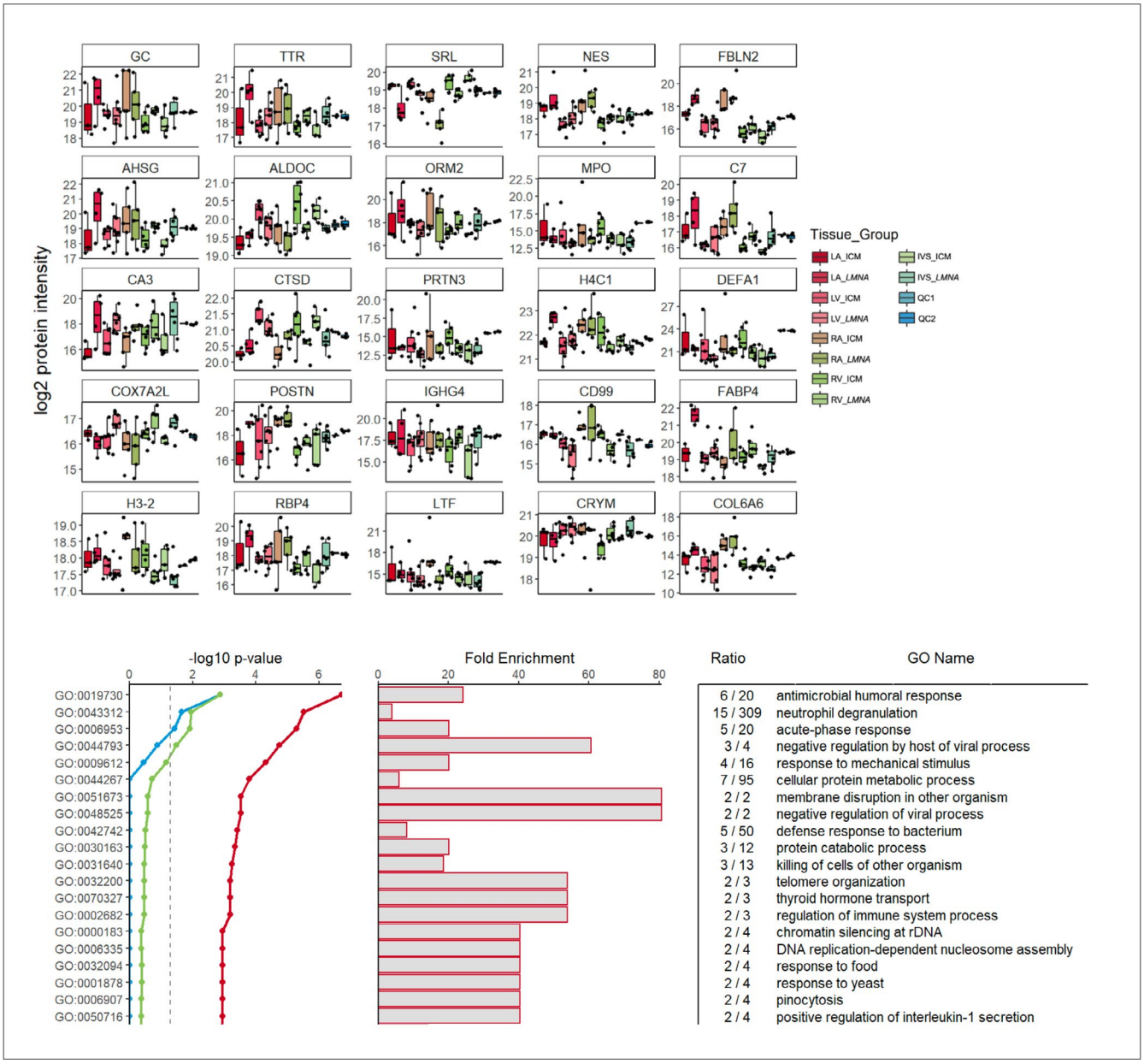

Supplementary Figure S3. Right ventricular myocardial proteins and their gene ontology. Box plots (**top panel**) comparing intensities of the top 25 differentially abundant RV proteins between LMNA and ICM based on *q*-value. The top 20 enriched biological processes across these 52 proteins are presented (**bottom panel**) along with enrichment *p*-values and fold enrichment.

Abbreviations as in Supplementary Figures S1 and 2.

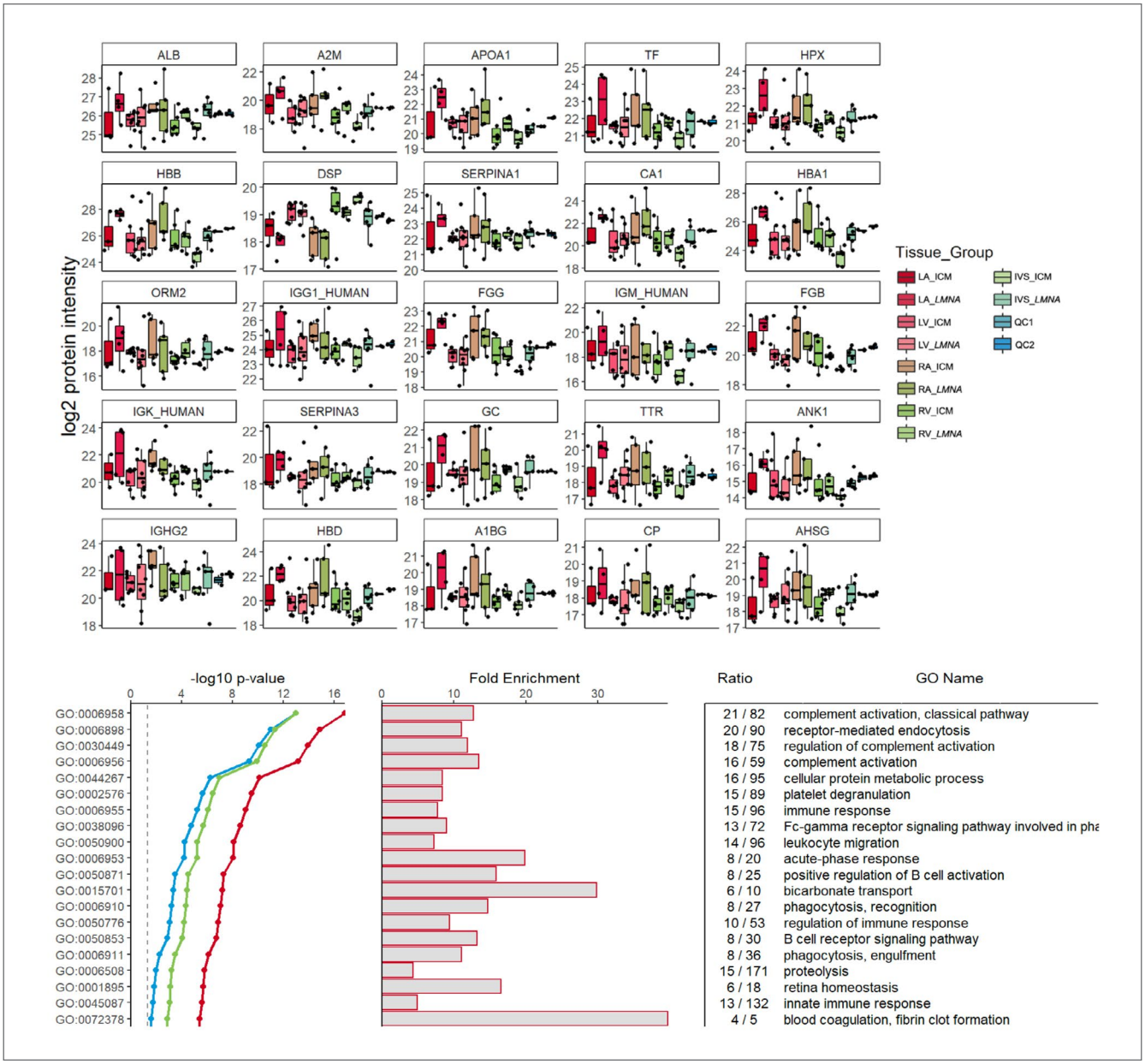

Supplementary Figure S4. Interventricular septal myocardial proteins and their gene ontology. Box plots (**top panel**) comparing intensities of the top 25 differentially abundant septal proteins between LMNA and ICM based on *q*-value. The top 20 enriched biological processes across these 85 proteins are shown (**bottom panel**) along with enrichment *p*-values and fold enrichment.

Abbreviations as in Supplementary Figure S1 and 2.